PTEP

Prog. Theor. Exp. Phys. **2024** 05B101 (13 pages)
DOI: 10.1093/ptep/ptae056

Neutrinos from Core-Collapse Supernova Explosions

Hideyuki Suzuki *

Department of Physics and Astronomy, Faculty of Science and Technology, Tokyo University of Science, Yamazaki 2641, Noda, Chiba 278-8510, Japan

*E-mail: suzukih@rs.tus.ac.jp

Received April 1, 2024; Revised April 3, 2024; Accepted April 24, 2024; Published April 25, 2024

The observation of supernova neutrinos from SN1987A by Kamiokande was an epoch-making event for both neutrino astronomy and supernova physics. Basic points in the standard pictures of stellar evolution and core-collapse supernovae were verified and research on them entered new advanced stages. In this article we give an overview of the supernova neutrinos emitted from core-collapse supernova explosions as well as the significance of their observations.

Subject Index E26, F22

1. Introduction

After the first years of the Kamioka Nucleon Decay Experiment, Prof. Koshiba directed the upgrade of Kamiokande to give the capability of observing $O(10)$ MeV neutrinos (solar neutrinos and supernova neutrinos) and the second phase of the experiment, Kamiokande-II, started in January 1987. It was exciting that the nearest supernova SN1987A since Kepler's supernova (SN1604) exploded in February 1987 and Kamiokande-II could observe 11 neutrinos from the core-collapse supernova (CCSN) for the first time in history [1]. Prof. Koshiba's foresight and leadership have borne fruit in the shape of neutrino astronomy. In this article we give an overview of our understanding of the supernova neutrinos to the research on which Prof. Koshiba made an unprecedented contribution, including the motivation for the subsequent progress.

To begin with, cosmic evolution can be understood as being driven by supernovae (Fig. 1). Stars are formed from interstellar matter with no or a small amount of heavy elements (metal) and then synthesize heavy elements in their lives and scatter them into interstellar space via supernovae and so on. This cycle has been repeated and the universe has evolved chemically. In addition, the evolution of stars depends on their initial masses and metallicities. Massive stars have higher central temperatures and nuclear fusion continues stably to form iron cores. The iron core can no longer generate further nuclear energy and therefore collapses gravitationally to form a neutron star or a black hole. The outer envelope often explodes as a core-collapse supernova (CCSN) but, in some cases, all stellar layers fall onto the central core without explosion: this is called a failed supernova. In both cases, copious neutrinos, called supernova neutrinos, are emitted. The amount and the energy spectra of supernova neutrinos emitted from a progenitor also depend on the progenitor mass and metallicity. The accumulated supernova neutrinos since the beginning of the universe

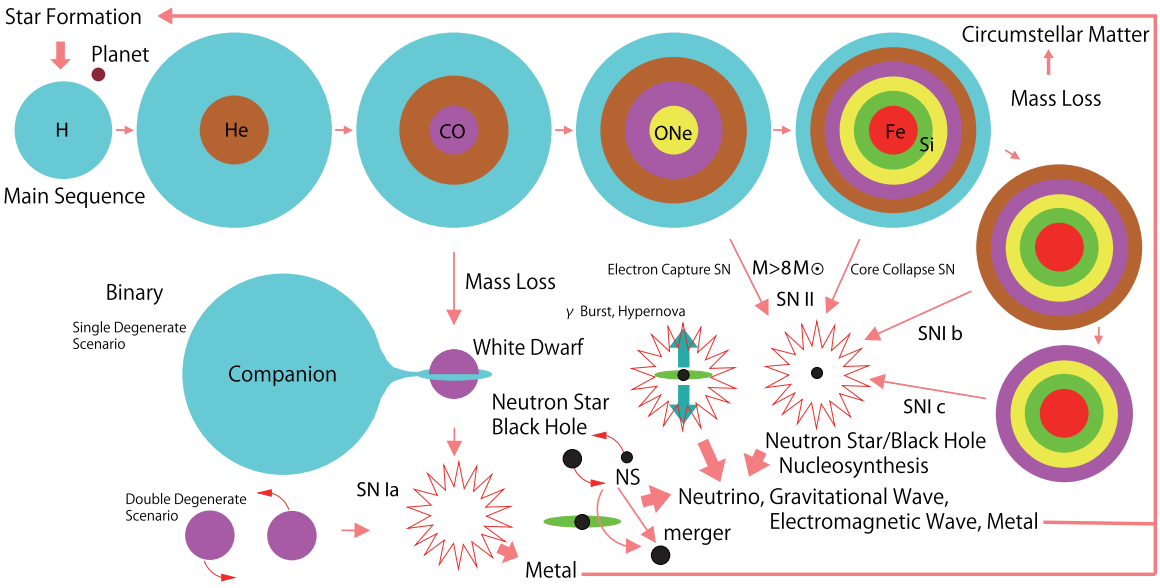

Fig. 1. Schematic picture of stellar evolution and supernova explosions.

constitute the diffuse supernova neutrino background (DSNB), which also represents cosmic evolution.

The importance of neutrinos in core-collapse supernovae can be understood as follows. In the collapsed supernova core (temperature $T \sim 10$ MeV, density $\rho_{\rm B} \gtrsim 10^{14}\ {\rm g\,cm^{-3}}$), the timescale for weak interactions is much shorter than the dynamical timescale of the core. Therefore, even neutrinos are trapped inside the core; they are also in thermal and chemical equilibrium with matter. While the number density of neutrinos becomes of the same order as the other particles ($n_\nu \sim n_\gamma \sim n_{\rm e} \sim n_{\rm B}$, γ: photons, e: electrons, B: baryons/nucleons), the mean free path of neutrinos is much longer than those of other particles ($\lambda_\nu \gg \lambda_\gamma, \lambda_{\rm e}, \lambda_{\rm B}$). As a result, neutrinos carry the energy and drive the evolution of the core. In fact, the observed energy of supernova explosions (kinetic and radiation) is $O(10^{51})$ erg while the gravitational energy released during neutron star formation (roughly equal to the binding energy of the neutron star) is $O(10^{53})$ erg. Neutrinos carry almost all the released energy, $E_{\nu\ {\rm tot}} \sim O(10^{53})$ erg. Furthermore, supernova cores can be seen by such neutrinos, so that core-collapse supernovae are an important target for the new neutrino astronomy.

All species of neutrinos ($\nu_{\rm e}$, $\bar{\nu}_{\rm e}$, ν_μ, $\bar{\nu}_\mu$, ν_τ, $\bar{\nu}_\tau$) are produced in core-collapse supernovae. The total energy emitted by $\nu_{\rm e}$ from the neutronization process that should occur during neutron star formation can be roughly estimated as $26\frac{M_{\rm Fe\ core}}{m_{\rm Fe}}\langle E_{\nu_{\rm e}}\rangle \sim 10^{52}\ {\rm erg}\frac{M_{\rm Fe\ core}}{1.4M_\odot}\frac{\langle E_{\nu_{\rm e}}\rangle}{10\ {\rm MeV}} \sim O(0.1) \times E_{\nu\ {\rm tot}}$, where $\langle E_{\nu_{\rm e}}\rangle \sim 10$MeV is the average energy of the emitted $\nu_{\rm e}$ and $M_{\rm Fe\ core}$, $m_{\rm Fe}$ are the masses of the Fe core and the Fe nucleus, respectively. This means that $\nu_{\rm e}$ from neutronization are minor and the majority are thermal neutrinos of all species. Meanwhile the temperature is less than the muon mass ($O(100)$ MeV) so that the number densities of μ and τ are negligible compared with the electron density ($n_{\rm e} \gg n_\mu, n_\tau$). Therefore, nonelectron-type neutrinos and antineutrinos cannot interact via the charged current channel and can be treated together as a representative neutrino species $\nu_{\rm x}$. Core-collapse supernovae are unique as the strong source of all types of neutrinos with energies around 10 MeV.

2. Scenario of core-collapse supernova explosions

Here we describe briefly the scenario of a core-collapse supernova explosion step by step (see Fig. 2). For more details, refer to Ref. [2]. As is well known, massive stars evolve to have an onion-like structure with the Fe core surrounded by Si, ONe, CO, and He shells and a H envelope if not lost by any mass loss mechanism. The Fe core no longer produces thermal energy by nuclear fusion because iron has the largest nuclear binding energy. At the beginning there is hydrostatic equilibrium between gravity and the pressure gradient by relativistic degenerate electrons (core mass $M_{\rm core} = 1$–$2M_\odot$, radius $R_{\rm core} = 10^8$–10^9 cm, density $\rho_{\rm B} = 10^9$–10^{10} g cm^{-3}, temperature $T = 0.1$–1 MeV, electron Fermi energy $\mu_{\rm e} \sim 10$ MeV $\gg T, m_{\rm e}$). As the core grows, it becomes unstable against gravitational collapse due to the electron capture and/or the photodissociation of heavy nuclei, both of which suppress the pressure increase accompanied by contraction.

At the onset of core collapse, $\nu_{\rm e}$ generated by electron capture ($e^- A(N, Z) \to \nu_{\rm e} A'(N+1, Z-1)$) can freely escape from the core; the mean free path λ_ν is larger than the core radius ($\lambda_\nu > R_{\rm core}$). The timescale of the core collapse can be estimated as the dynamical timescale $\tau_{\rm dyn} \sim \sqrt{1/G\rho_{\rm B}} \sim O(10^2)$ ms.

When the density exceeds $O(10^{11})$ g cm^{-3}, the neutrino mean free path falls below the core radius ($\lambda_\nu < R_{\rm core}$) and the core becomes opaque for neutrinos. In other words, at that time, the neutrinosphere appears. Inside the neutrinosphere it is opaque for neutrinos and one can regard it as the surface for neutrinos. Furthermore, the diffusion timescale for neutrinos to escape from the core $\tau_{\rm diff} \sim \frac{R_{\rm core}^2}{c\lambda_\nu}$ becomes longer than the dynamical timescale when the density exceeds $O(10^{12})$ g cm^{-3}: neutrinos cannot escape from the core during the collapse, i.e. neutrino trapping. In the collapsing core, the main opacity source for neutrinos is coherent scattering off heavy nuclei ($\nu_{\rm e} A \to \nu_{\rm e} A$) whose cross section is proportional to the square of the mass number and the square of the neutrino energy (cross section $\sigma \propto A^2 E^2$ where A, E are the mass number of nuclei and the neutrino energy, respectively). This is because the neutrino wavelength is larger than the nuclear radius $\propto A^{1/3}$.

The neutrino trapping was pointed out by Sato [3] and has positive feedback. Once the neutrinos are trapped, they become degenerate and their Fermi energy (E_F) increases. This results in larger cross sections to prevent escapes. Due to Pauli blocking, degenerate neutrinos also suppress further electron capture, neutronization of nuclei, and neutron drip from neutronized nuclei, leading to survival of heavy nuclei and keeping the core opaque for neutrinos. This positive feedback is shown in Fig 3.

If there is no neutrino trapping, emission of supernova neutrinos lasts only for $O(100)$ ms; the core would bounce at lower density due to the free neutron pressure and the strong shock wave could not be launched because of insufficient collapse.

When the density exceeds nucleon density ($O(10^{14})$ g cm^{-3}), the repulsive part of the nuclear force stiffens the inner core abruptly. The subsonic inner core (less massive than $1M_\odot$) bounces simultaneously to be in new hydrostatic equilibrium (proto-neutron star: PNS) and, near the boundary between the bounced inner core and the supersonically falling outer core, the shock wave is launched. The initial shock energy can be estimated as gravitational energy released from the bounced inner core (several times 10^{51} erg). This is sufficient for the observed supernova explosion if there is no loss of shock energy.

As the shock wave propagates outwards, heavy nuclei in the shock-passing region are dissociated to become free nucleons and the extra electron capture proceeds because free protons have

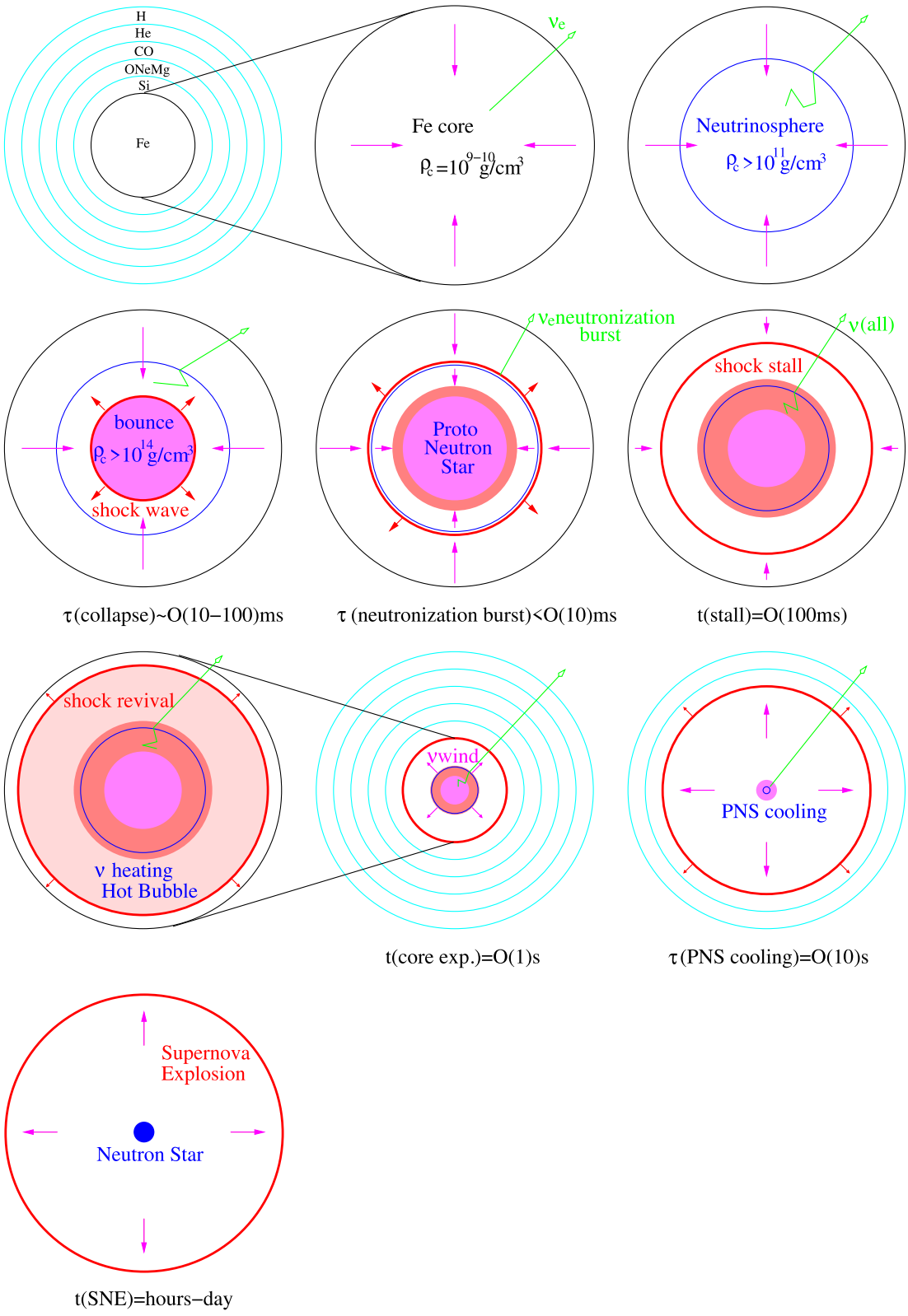

Fig. 2. Scenario of a core-collapse supernova explosion.

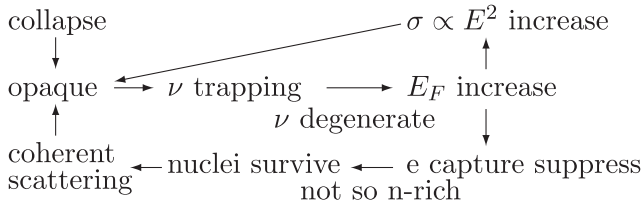

Fig. 3. Schematic figure about the positive feedback of neutrino trapping.

a larger capture rate than nuclei. Until the shock wave passes the neutrinosphere, the emitted ν_e are trapped inside the neutrinosphere. However, when the shock wave passes through the neutrinosphere, ν_e produced by the electron capture are no longer trapped and can escape simultaneously. This is the neutronization burst of ν_e that lasts for $O(10)$ ms, which is the crossing timescale of the shock wave around the neutrinosphere.

In this way, the shock wave loses energy by dissociation of heavy nuclei and by neutrino emission. Except for light core stars, the shock wave first stalls on the way to the core surface. The rapidly falling matter of the outer core collide with the shock wave; the kinetic energy is transformed into thermal energy and accretes slowly onto the hydrostatic inner core (proto-neutron star). Thus, the proto-neutron star grows to have a hot mantle above an unshocked inner core.

Inside the proto-neutron star, the timescale for weak interaction is sufficiently short for neutrinos of all species to be in β-equilibrium. In addition to ν_e from electron capture, other neutrinos are emitted from positron capture ($e^+n \to \bar{\nu}_e p$) and electron–positron pair annihilation ($e^-e^+ \to \nu\bar{\nu}$) in the hot shocked region.

For the moment of the neutrino observation of SN1987A, the delayed explosion model in which the stalled shock wave could revive due to neutrino heating of the hot bubble beneath the shock front is discussed in spherically symmetric cases [4]. Meanwhile, electromagnetic observations of SN1987A revealed several aspherical features of the supernova explosion and multidimensional simulations of supernova explosions were performed after that. Currently, it is under discussion whether convection inside the proto-neutron star (PNS convection), convection in gain regions just beneath the shock front where neutrino heating occurs (neutrino convection), and the standing accretion shock instability (SASI) might be keys to successful explosions. PNS convection enhances the neutrino luminosity and neutrino convection conveys the heated matter to just the beneath of the stalled shock front. If SASI occurs, the advection timescale for the accreting matter across the gain region could become longer than the neutrino heating timescale necessary for the matter to obtain sufficient energy to be ejected to infinity.

Multidimensional simulations show that the stalled shock can revive to explode the core in 0.1–1 s. Since the overlying envelope is loosely bounded, the shock wave will succeed the stellar explosion without obstacles once the shock wave can pass through the core.

Optical stellar explosion occurs at the shock breakout of the photosphere and it is delayed by several minutes or hours from the core explosion.

After the core explosion, matter accretion onto the proto-neutron star ceases. Subsequently the proto-neutron star cools and deleptonizes (loses its total lepton number) while emitting neutrinos on the diffusion timescale of neutrinos (10–100 s). In Fig. 4, we show the inner structures of a proto-neutron star during the cooling phase [5]. The central entropy first increases due to the heat flux from the hotter mantle conveyed by $\bar{\nu}_e$ and ν_x. While almost all neutrinos diffuse

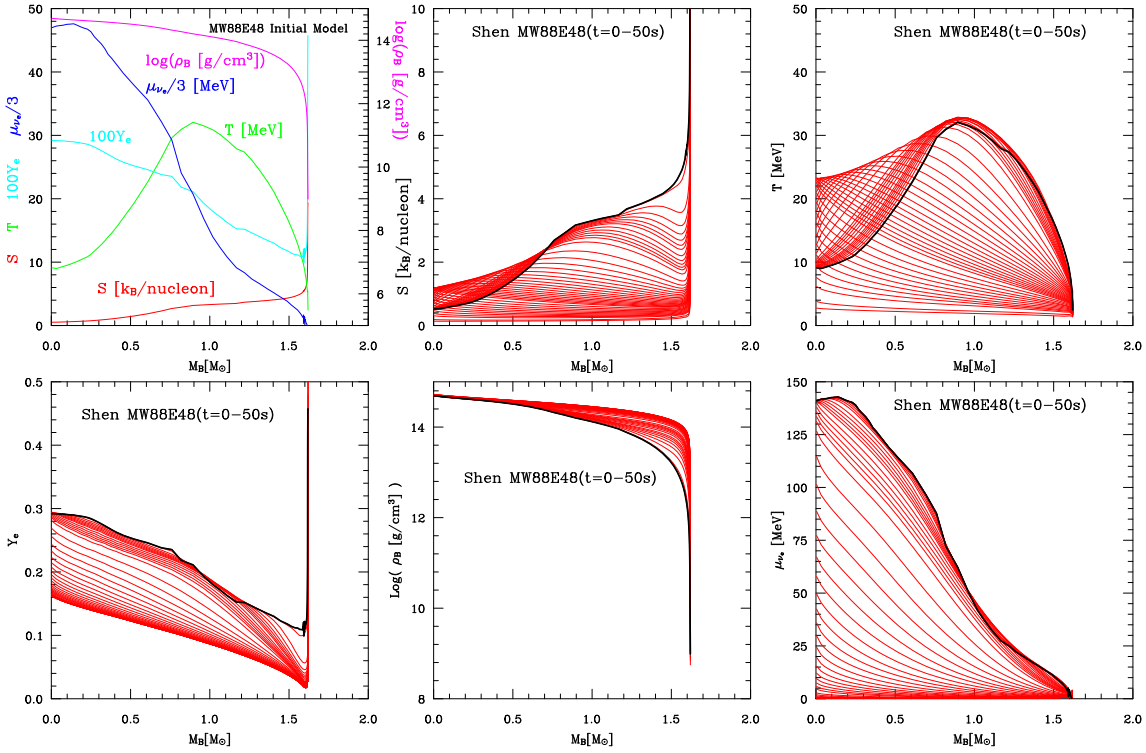

Fig. 4. Time evolution of the inner profiles of a proto-neutron star (model MW88E48). The upper left panel shows the initial profiles of density $\rho_{\rm B}$, temperature T, electron fraction $Y_{\rm e}$, entropy S, and neutrino chemical potential $\mu_{\nu_{\rm e}}$ defined as $\mu_{\rm p} + \mu_{\rm e} - \mu_{\rm n}$. The other five panels show snapshots up to 50 s. The black lines depict the initial profiles.

out until 50 s (the chemical potential of the $\nu_{\rm e}$ drops to 0), the electron fraction $Y_{\rm e}$ remains still larger than 0.1 at the center. This $Y_{\rm e}$ profile corresponds to the neutrinoless β-equilibrium in an ordinary cool neutron star that depends on the nuclear EOS. In this model, we adopt the EOS of Shen et al. [6] as the nuclear EOS.

2.1. *Three phases of supernova neutrinos*

Supernova neutrinos can be divided roughly into three phases without clear boundaries. The first phase is the core-collapse and bounce phase including the neutronization burst of $\nu_{\rm e}$. The timescale is less than 100 ms and $\nu_{\rm e}$ due to electron capture are dominant. Although the peak luminosity of the neutronization burst exceeds 10^{53} erg s^{-1}, the total $\nu_{\rm e}$ energy is $O(10^{51})$ erg because of the short duration.

The second phase is the accretion phase lasting $O(1)$ s until the core explosion. The shock wave first stalls and then revives. All types of neutrinos are emitted from the accreted matter and diffuse out from the inner core. The total neutrino energy is $\int L_\nu dt = O(10^{53})$ erg.

Note that there exists a hierarchy of average energy($O(10)$ MeV) among the three types of neutrinos. Since $\nu_{\rm e}$ interact with matter containing electrons via both charged current and neutral current, the mean free path $\lambda_{\nu_{\rm e}}$ is the shortest among the three ($\lambda_{\nu_{\rm e}} < \lambda_{\bar{\nu}_{\rm e}} < \lambda_{\nu_{\rm x}}$). Consequently, the neutrinosphere for $\nu_{\rm e}$ locates outermost ($R_{\nu_{\rm e}} > R_{\bar{\nu}_{\rm e}} > R_{\nu_{\rm x}}$) and the temperature at the neutrinosphere is the lowest ($T_{\nu_{\rm e}} < T_{\bar{\nu}_{\rm e}} < T_{\nu_{\rm x}}$). This results in the hierarchy of the average energies: $\langle\omega_{\nu_{\rm e}}\rangle < \langle\omega_{\bar{\nu}_{\rm e}}\rangle < \langle\omega_{\nu_{\rm x}}\rangle$.

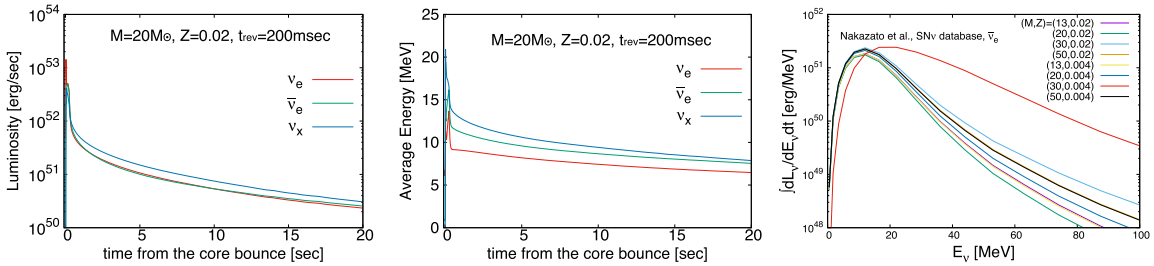

Fig. 5. Left and middle panels: Evolution of luminosity and average energy of supernova neutrinos. Right panel: Time-integrated energy spectra of $\bar{\nu}_e$ for various progenitors. Data are taken from our supernova neutrino database [7].

In this phase the neutrino luminosity might have correlations with the matter accretion rate because the gravitational energy released by the accreted matter converts into thermal energy and, in turn, neutrino luminosity. A sudden decrease of the neutrino luminosity might indicate shock revival or core explosion.

The third phase is the proto-neutron star cooling phase. After the core explosion, a proto-neutron star with a radius of several tens of km and a proton fraction of about 0.3 cools and deleptonizes while emitting neutrinos to become an ordinary cool neutron star with a radius of around 10 km and a proton/electron fraction of around 0.1. It takes 10–100 s for neutrinos to diffuse out and the total energy amounts to $O(10^{53})$ erg. In the less hot region with a small amount of positrons, the nucleon bremsstrahlung processes NN $\rightarrow$ NN$\nu\bar{\nu}$ act as the main source for $\bar{\nu}_e$ and ν_x.

It is worth noting that, as the proto-neutron star cools and neutronizes, the differences in the average energies of the three types of neutrinos tend to disappear. This is because the neutron-rich matter interacts with $\bar{\nu}_e$ and ν_x almost equally and because the degeneracy of electrons, protons, and neutrons prohibits ν_e interactions, too.

In Fig. 5, typical neutrino luminosities and average energies as functions of post-bounce time are shown. Typical $\bar{\nu}_e$ time-integrated energy spectra (including a black-hole forming case: $M = 30M_\odot$, $Z = 0.004$) are also shown. These results are taken from our supernova neutrino database [7].

3. Observation of supernova neutrinos from SN1987A

On 24 February 1987, a core-collapse supernova (SN1987A) was discovered optically [8] in the Large Magellanic Cloud. It was the nearest supernova recorded since the galactic supernova SN1604 and the first supernova observed in 1987. The Kamiokande-II Collaboration analyzed their data of the preceding days and found 11 events caused by the neutrino burst from SN1987A on 23 February 1987, 7:35:35 UT($\pm$1 min) [1,9]. The IMB Collaboration also noted the detection of the neutrino burst (8 events [10]) from SN1987A subsequently. The exciting days around the observation of supernova neutrinos from SN1987A are described in Ref. [11]. We present a simple analysis of the data observed by the two water Cerenkov detectors (taken from Ref. [12]).

The data for the neutrino events observed by the two detectors are summarized in Table 1. Since the Kamiokande-II detector had just completed the refinement for the observation of solar neutrinos in addition to nucleon decay experiments, it observed lower-energy events. The detection efficiencies of electrons/positrons η_{detector} in each detector are shown in Fig. 6 [9,13].

Table 1. Summary of the observations of the neutrino burst. The event time is measured from the first event at 7:35:35±1 min UT for Kamiokande-II and 7:35:41.374 UT for IMB. The event angle is given with respect to the direction away from SN1987A. The $\bar{\nu}_e$ energy for IMB is estimated assuming that events are due to $\bar{\nu}_e p \to e^+ n$. The quoted errors in the energy do not include the systematic error related to energy calibration. Event $*$ in the Kamiokande-II data is regarded as a background event due to its energy being lower than the threshold.

Kamiokande-II				IMB				
Event	Event time (s)	$e^{\pm}$ energy (MeV)	$e^{\pm}$ angle (deg)	Event	Event time (s)	$e^{\pm}$ energy (MeV)	$e^{\pm}$ angle (deg)	$\bar{\nu}_e$ energy (MeV)
1	0.000	20.0 ± 2.9	18 ± 18	1	0.000	38 ± 7	80 ± 10	41 ± 7
2	0.107	13.5 ± 3.2	40 ± 27	2	0.412	37 ± 7	44 ± 15	39 ± 7
3	0.303	7.5 ± 2.0	108 ± 32	3	0.650	28 ± 6	56 ± 20	30 ± 6
4	0.324	9.2 ± 2.7	70 ± 30	4	1.141	39 ± 7	65 ± 20	42 ± 7
5	0.507	12.8 ± 2.9	135 ± 23	5	1.562	36 ± 9	33 ± 15	38 ± 9
$*$	0.686	6.3 ± 1.7	68 ± 77	6	2.684	36 ± 6	52 ± 10	38 ± 6
6	1.541	35.4 ± 8.0	32 ± 16	7	5.010	19 ± 5	42 ± 20	21 ± 5
7	1.728	21.0 ± 4.2	30 ± 18	8	5.582	22 ± 5	104 ± 20	24 ± 5
8	1.915	19.8 ± 3.2	38 ± 22					
9	9.219	8.6 ± 2.7	122 ± 30					
10	10.433	13.0 ± 2.6	49 ± 26					
11	12.439	8.9 ± 1.9	91 ± 39					

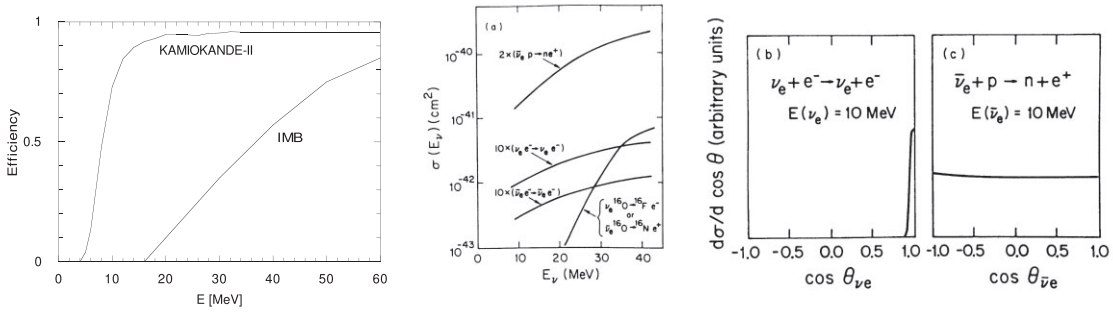

Fig. 6. Left panel: Detection efficiencies of the Kamiokande-II and IMB detectors. In these curves, the dead time effect is not taken into account. Middle panel: Cross sections for typical neutrino interactions in a water Cerenkov detector as a function of incident neutrino energy. Right panel: Angular differential cross section for the two interactions: $\nu_e e^- \to \nu_e e^-$ (b) and $\bar{\nu}_e p \to e^+ n$ (c). (Taken from K. S. Hirata et al. [9], "Observation in the Kamiokande-II detector of the neutrino burst from supernova SN1987A", Phys. Rev. D38, 448 (1988) Fig.14, by permission of American Physical Society. This figure is not covered by the terms of the Creative Commons licence of this publication. For permission to reuse, please contact American Physical Society.)

We adopt the central values of the reported efficiency of the IMB detector. The fiducial volumes $V_{\rm detector}$ are 2140 m^3 for Kamiokande-II and 6800 m^3 for IMB, respectively. In addition, we multiply the detection efficiency of the IMB detector by a factor of 0.87 because IMB reported dead time of 13% during the burst. On the other hand, the Kamiokande-II detector was almost free of dead time.

The expected number of events for each neutrino interaction channel in each detector with electron/positron energy E_e and event angle θ_e per unit energy per unit $\cos\theta_e$ per unit time,

$d^3N_{\rm expect}/dE_{\rm e}d\cos\theta_{\rm e}dt$, can be expressed as

$$\frac{d^3N_{\rm expect}^{\rm detector\ (i)}(E_{\rm e},\cos\theta_{\rm e},t)}{dE_{\rm e}d\cos\theta_{\rm e}dt} = n_{\rm target}^{(i)}V_{\rm detector}\eta_{\rm detector}(E_{\rm e}) \times \frac{1}{4\pi d_{\rm SN}^2}\frac{d^2N_\nu(E_\nu,t)}{dE_\nu dt}\frac{d\sigma^{(i)}(E_\nu,\cos\theta_{\rm e})}{d\cos\theta_{\rm e}}\Big/\frac{dE_{\rm e}^{(i)}(E_\nu,\cos\theta_{\rm e})}{dE_\nu} \quad (1)$$

where the superscript (i) denotes the interaction channel such as $\bar{\nu}_{\rm e}{\rm p}\to{\rm ne}^+$ or $\nu{\rm e}^-\to\nu{\rm e}^-$, $n_{\rm target}^{(i)}$ is the number density of the targets for the interaction (i) in water ($n_{\rm p}=2\times\rho_{\rm H_2O}/m_{\rm H_2O}$,$n_{\rm e^-}=10\times\rho_{\rm H_2O}/m_{\rm H_2O}$, where $\rho_{\rm H_2O}$ is the density of the water and $m_{\rm H_2O}$ is the mass of a water molecule), $d_{\rm SN}=50$ kpc is the distance to the supernova, $d^2N_\nu/dE_\nu dt$ is the neutrino number emitted from the supernova per unit energy per unit time, and $d\sigma^{(i)}/d\cos\theta_{\rm e}$ is the differential cross section for the interaction (i). Note that for neutrinos with energies of 10–30 MeV the $\bar{\nu}_{\rm e}$ absorption by protons (the inverse beta decay, $\bar{\nu}_{\rm e}{\rm p}\to{\rm ne}^+$) has the largest $n_{\rm target}\sigma$; second is the electron scattering of $\nu_{\rm e}$: $\nu_{\rm e}{\rm e}^-\to\nu_{\rm e}{\rm e}^-$ (see Fig. 6).

Analysis of the observed data shows that they are consistent with the standard picture of supernova neutrinos even with small statistics as follows (see Ref. [14] for a recent analysis).

Duration time of the neutrino burst. The neutrino burst was observed during time spans of 12.4 s in Kamiokande-II and 5.6 s in IMB, respectively. This timescale is consistent with the neutrino diffusion timescale of the supernova core, which is evidence for neutrino trapping, in which neutrinos are first trapped in the supernova core and then diffuse out.

Angular distribution of the observed positrons/electrons. Roughly speaking, most of the supernova neutrinos are emitted thermally and all types of neutrinos are emitted equally. As shown in Fig. 6, the inverse beta decay (IBD) process ($\bar{\nu}_{\rm e}{\rm p}\to{\rm e}^+{\rm n}$) dominates other scattering processes ($\nu{\rm e}^-\to\nu{\rm e}^-$) in water at neutrino energies around 10 MeV. As for IBD, the angular distribution of the emitted positrons is nearly isotropic while the scattered electrons have a sharp forward peak. This is because the protons (targets of IBD) are heavy and electrons (targets of electron scattering) are light.

Consequently, the angular distribution of the supernova neutrino events in water is expected to be nearly isotropic. Among the 19 (11 + 8) events, there was only one event (the first event of Kamiokande-II) in the forward direction. This is consistent with the expected ratio of the scattering events to the IBD events. For example, it is evaluated to be about 0.05 based on numerical results by Mayle (model 15C [15]). Thus, the observed angular distribution is consistent with the standard picture of supernova neutrinos in which all types of neutrinos are emitted roughly equally.

Neutronization burst. As mentioned before, the so-called neutronization burst of $\nu_{\rm e}$ is emitted at the shock breakout of the neutrinosphere. Free protons produced by the nuclear dissociation capture electrons and emit $\nu_{\rm e}$. The timescale of the neutronization burst is very short (less than 10 ms) and the total energy of $\nu_{\rm e}$ emitted during the neutronization burst is of the order of 10^{51} erg. Numerical simulations predict that the number of scattering events corresponding to the neutronization burst is less than 0.1 [16]. While the first event of Kamiokande-II could be interpreted as a $\nu_{\rm e}$ scattering event due to its forward direction, the small statistics prevent us from concluding that it really is a scattering event caused by the neutronization burst. Therefore, we assume that the 19 observed events are all due to $\bar{\nu}_{\rm e}{\rm p}\to{\rm e}^+{\rm n}$.

The average and total energy of $\bar{\nu}_{\rm e}$ flux. Although it is not precise, as the zeroth-order approximation, the energy spectrum of supernova neutrinos can be regarded as a thermal

(Fermi–Dirac) spectrum with a temperature (T) and a vanishing chemical potential. When we denote the time-integrated luminosity (total energy) of $\bar{\nu}_e$ as $E_{\mathrm{tot},\bar{\nu}_e}$, the time-integrated neutrino number spectrum can be expressed as

$$\int \frac{d^2N_\nu}{dE_\nu dt} dt = \frac{E_{\mathrm{tot},\bar{\nu}_e}}{\int_0^\infty \frac{E_\nu^3}{e^{E_\nu/T}+1} dE_\nu} \frac{E_\nu^2}{e^{E_\nu/T}+1}. \tag{2}$$

Using Eqs. (1) and (2), we can estimate various observational quantities expected for this simplified model. Comparison of the expected number of events and the average energy of events with observed data puts constraints on the values of T and $E_{\mathrm{tot},\bar{\nu}_e}$. For example, we can apply the maximum likelihood method to the combined data from the two detectors as follows. The expected number of events and the expected average energy of events for each detector can be calculated as

$$N_{\mathrm{expect}}^{\mathrm{detector}} = \int \frac{d^3N_{\mathrm{expect}}^{\mathrm{detector}}(E_e, \cos\theta_e, t)}{dE_e d\cos\theta_e dt} dE_e d\cos\theta_e dt \tag{3}$$

$$\langle E_{\mathrm{expect}}^{\mathrm{detector}} \rangle = \int E_e \frac{d^3N_{\mathrm{expect}}^{\mathrm{detector}}(E_e, \cos\theta_e, t)}{dE_e d\cos\theta_e dt} dE_e d\cos\theta_e dt \Big/ N_{\mathrm{expect}}^{\mathrm{detector}}. \tag{4}$$

Meanwhile, the nonmonochromatic neutrino flux causes intrinsic fluctuation of the event energy $\sigma_{\mathrm{expect}}^{\mathrm{detector}}$ as

$$(\sigma_{\mathrm{expect}}^{\mathrm{detector}})^2 = \int (E_e - \langle E_{\mathrm{expect}}^{\mathrm{detector}} \rangle)^2 \frac{d^3N_{\mathrm{expect}}^{\mathrm{detector}}(E_e, \cos\theta_e, t)}{dE_e d\cos\theta_e dt} dE_e d\cos\theta_e dt \Big/ N_{\mathrm{expect}}^{\mathrm{detector}}. \tag{5}$$

Since the distribution of the number of events in each detector can be considered as a Poisson distribution with mean $N_{\mathrm{expect}}^{\mathrm{detector}}$ and the distribution of the average energy of $N_{\mathrm{obs}}^{\mathrm{detector}}$ events ($N_{\mathrm{obs}}^{\text{Kamiokande-II}} = 11$, $N_{\mathrm{obs}}^{\mathrm{IMB}} = 8$) can be regarded as a normal distribution with mean $\langle E_{\mathrm{expect}}^{\mathrm{detector}} \rangle$ and variance

$$\sigma^{\mathrm{detector}} = \sqrt{\frac{(\sigma_{\mathrm{expect}}^{\mathrm{detector}})^2}{N_{\mathrm{obs}}^{\mathrm{detector}}} + (\sigma_{\mathrm{obs}}^{\mathrm{detector}})^2} \tag{6}$$

where $\sigma_{\mathrm{obs}}^{\mathrm{detector}}$ is the error in the average energy of observed events including the detector's systematic error ($\sigma_{\mathrm{obs}}^{\text{Kamiokande-II}} = 1.9\,\mathrm{MeV}$, $\sigma_{\mathrm{obs}}^{\mathrm{IMB}} = 5.6\,\mathrm{MeV}$), the joint likelihood function $L(T, E_{\mathrm{tot},\bar{\nu}_e})$ is defined as

$$L(T, E_{\mathrm{tot},\bar{\nu}_e}) = \prod_{\mathrm{detector}} \frac{1}{\sqrt{2\pi}\sigma^{\mathrm{detector}}} \exp\left[-\frac{1}{2} \left(\frac{\langle E_{\mathrm{obs}}^{\mathrm{detector}} \rangle - \langle E_{\mathrm{expect}}^{\mathrm{detector}} \rangle}{\sigma^{\mathrm{detector}}} \right)^2 \right] \times \frac{(N_{\mathrm{expect}}^{\mathrm{detector}})^{N_{\mathrm{obs}}^{\mathrm{detector}}} \exp(-N_{\mathrm{expect}}^{\mathrm{detector}})}{(N_{\mathrm{obs}}^{\mathrm{detector}})!}, \tag{7}$$

where $\langle E_{\mathrm{obs}}^{\mathrm{detector}} \rangle$ is the average energy of observed events ($\langle E_{\mathrm{obs}}^{\text{Kamiokande-II}} \rangle = 15.4\,\mathrm{MeV}$, $\langle E_{\mathrm{obs}}^{\mathrm{IMB}} \rangle = 32.8\,\mathrm{MeV}$). A parameter set that maximizes this likelihood function consists of the best-fitting parameters for reproducing the observed data of the two detectors simultaneously. Our evaluated parameters are $T = 4.0 \pm 0.5\,\mathrm{MeV}$ and $E_{\mathrm{tot},\bar{\nu}_e} = 3.4^{+1.4}_{-1.0} \cdot 10^{52}\,\mathrm{erg}$. These temperature and total energy of the $\bar{\nu}_e$ are in the range predicted by various supernova simulations.

The total energy carried by all species of neutrinos (E_{tot}) is nearly equal to the binding energy of the remaining neutron star (E_{bind}). We can estimate the former from the observed data of the

neutrino burst and we can estimate the mass of the neutron star just born in SN1987A using the relation between the neutron star mass and its binding energy.

$E_{\rm bind} \sim E_{\rm tot}$ can be evaluated as six times the total energy emitted as $\bar{\nu}_{\rm e}$ ($E_{{\rm tot},\bar{\nu}_{\rm e}}$) to be in the range of 1.4–$2.9 \cdot 10^{53}$ erg.

The relation between the neutron star mass and its binding energy depends on the nuclear equation of states. Our previous study [17] considered a rather old set of equations of states and concluded that the neutron star mass is in the range of 1.0–$1.7 M_\odot$. These days, after the discovery of heavier neutron stars ($M \gtrsim 2M_\odot$) and after the observation of gravitational waves from a neutron star merger, a soft equation of states is disfavored. It seems that a black hole was not formed in SN1987A.

Time evolution. Since the observed neutrino events for SN1987A had small statistics, we cannot know in detail the time evolution of the neutrino burst. However, one can see that higher-energy events concentrate in the first 3 s and that the event frequency becomes low at $t > 3$ s. This feature can be naturally interpreted as corresponding to cooling of the proto-neutron star.

Implications for particle physics. In spite of the small statistics of the neutrino events, there are a large number of implications for particle physics. Since it is beyond the scope of this article to follow all such implications, some topics will be picked up shortly.

What makes neutrinos important agents in the supernova core is their suitable coupling strength with matter. Neutrinos are produced copiously and hold substantial parts of the energy in the supernova core due to coupling that is not too weak. On the other hand, they escape from the core most rapidly among the constituents (nucleons, leptons, and photons) due to their weaker coupling with matter than other particles. Coupling that is too weak would prevent their production and coupling that is too strong would prevent their escape. If there exist other exotic particles with similar coupling strengths with matter, they must also have been produced and emitted from SN1987A as well as the observed neutrinos. The existence of such exotic particles should alter the feature of the supernova neutrino burst, e.g. leading to smaller number of neutrino events or a shorter time duration of the neutrino burst than predicted from the standard model of supernova neutrinos without exotic particles. The agreement between the standard prediction and the observation of neutrinos from SN1987A, conversely, put constraints on the existence and properties of such exotic particles.

In addition, the neutrino mass could be investigated by analyzing the dispersion of the time of flight from the supernova to the Earth; higher-energy neutrinos would fly faster than lower-energy neutrinos.

Since all types of neutrinos are emitted with spectral variations (e.g. the hierarchy of average energies) and with temporal variations (e.g. the neutronization burst), neutrino oscillation might have an influence on the explosion itself and on the observation on the Earth. However, compared with 30 years ago, the expected spectral differences among neutrino species are smaller so that the detection of oscillation effects becomes more difficult.

4. Summary and future prospects

Kamiokande, led by Prof. Koshiba, detected supernova neutrinos emitted from SN1987A and provided us with an invaluable opportunity to progress the supernova studies even with 11 neutrino events. The succeeding experiment, Super-Kamiokande, could detect $O(10^4)$ neutrinos from galactic supernovae so that the details of supernova explosion can be investigated. Furthermore, Hyper-Kamiokande, with a volume of eight times that of Super-Kamiokande,

is under construction. Core-collapse events that lead to black-hole (BH) formation also emit copious neutrinos. Observation of supernova neutrinos including BH formation cases would provide us with fruitful information concerning particle physics, nuclear physics, and astrophysics.

Aside from the neutrino burst from a single core-collapse event, supernova relic neutrinos (SRN) or diffuse supernova neutrino background (DSNB) are being extensively studied [18]. These are supernova neutrinos accumulated since the beginning of the universe. Their current fluxes and spectra are related to supernova rate and neutrino spectra emitted from various progenitors (mass and metallicity) and cosmic expansion law as follows:

$$\frac{dF_\nu(E_\nu, t_0)}{dE_\nu} = c\int_0^{t_0}\int_{M_{\rm min}}^{M_{\rm max}}\int_0^{Z_{\rm max}} \frac{d^2R_{\rm CC}(z, M, Z)}{dMdZ} dZdM \frac{dN_\nu(E'_\nu, M, Z)}{dE'_\nu}\frac{dE'_\nu}{dE_\nu}dt \tag{8}$$

$$dt = -\frac{dz}{(1+z)H(z)},\ dE'_\nu = (1+z)dE_\nu$$

where $R_{\rm CC}(z, M, Z)$ is the core-collapse supernova rate related to the star formation rate (SFR), initial mass function (IMF), and metallicity evolution; $\frac{dN_\nu(E'_\nu, M, Z)}{dE'_\nu}$ is the energy spectrum from an individual supernova progenitor with mass M and metallicity Z; E'_ν is the neutrino energy at the explosion; E_ν is the current (redshifted by cosmic expansion) neutrino energy; z is the redshift parameter; and $H(z)$ is the Hubble parameter.

Super-Kamiokande (now SK-Gd) [19] and KamLAND [20] continue to perform experiments aiming for the observation of SRN/DSNB and the first detection is expected within years. When observed, it should provide valuable combined information on supernova neutrinos, the core-collapse event rate, the star formation rate, the stellar initial mass function, the metallicity evolution, cosmic expansion, and so on. For more details, refer to Ref. [21].

Acknowledgments

The author thanks K. Sato, Y. Totsuka, and M. Koshiba for instructions into research on supernova neutrinos. He also thanks K. Nakazato for collaborations to make up the supernova neutrino database. This work was partially supported by JSPS Grants-in-Aid for Scientific Research on Innovative Areas "Unraveling the History of the Universe and Matter Evolution with Underground Physics" (No. 19H05802 and No. 19H05811) and for Transformative Research Areas "The creation of multi-messenger astrophysics" (No. 24H01817).

Conflict of interest statement. None declared.

References

[1] K. Hirata et al., Phys. Rev. Lett. **58**, 1490 (1987).
[2] S. Yamada, H. Nagakura, R. Akaho, A. Harada, S. Furusawa, W. Iwakami, H. Okawa, H. Matsufuru, and K. Sumiyoshi, Proc. Jpn. Acad. Ser. B **100**, 190 (2024).
[3] K. Sato, Prog. Theor. Phys. **53**, 595 (1975).
[4] H. A. Bethe and J. R. Wilson, Astrophys. J. **295**, 14 (1985).
[5] H. Suzuki, H. Kogure, F. Tomioka, K. Sumiyoshi, S. Yamada, and H. Shen, Nucl. Phys. A **718**, 703c (2003).
[6] H. Shen, H. Toki, K. Oyamatsu, and K. Sumiyoshi, Nucl. Phys. A **637**, 435 (1998).
[7] K. Nakazato, K. Sumiyoshi, H. Suzuki, T. Totani, H. Umeda, and S. Yamada, Astrophys. J. Suppl. **205**, 2 (2013).
[8] International Astronomical Union, IAU Circular No. 4316 (1987). http://www.cbat.eps.harvard.edu/iauc/04300/04316.html.
[9] K. S. Hirata et al., Phys. Rev. D **38**, 448 (1988).
[10] R. M. Bionta et al., Phys. Rev. Lett. **58**, 1494 (1987).

[11] M. Koshiba, Phys. Rep. **220**, 229 (1992).
[12] H. Suzuki, in Physics and Astrophysics of Neutrinos, eds. M. Fukugita and A. Suzuki (Springer, Tokyo, 1994), p.763.
[13] C. B. Bratton et al., Phys. Rev. D **37**, 3361 (1988).
[14] D. F. G. Fiorillo, M. Heinlein, H.-T. Janka, G. Raffelt, E. Vitagliano, and R. Bollig, Phys. Rev. D **108**, 083040 (2023).
[15] R. W. Mayle, Physical Processes in Collapse Driven Supernova, Ph.D. Thesis, University of California, Berkeley (1985).
[16] K. Sato and H. Suzuki, Phys. Rev. Lett. **58**, 2722 (1987).
[17] K. Sato and H. Suzuki, Phys. Lett. B **196**, 267 (1987).
[18] K. Nakazato, E. Mochida, Y. Niino, and H. Suzuki, Astrophys. J. **804**, 75 (2015).
[19] K. Abe et al., Phys. Rev. D **104**, 122002 (2021).
[20] S. Abe et al., Astrophys. J. **925**, 14 (2022).
[21] S. Ando, N. Ekanger, S. Horiuchi, and Y. Koshio, Proc. Jpn. Acad. Ser. B **99**, 460 (2023).